



PTMS Measurements of Radioactive Isotopes for Atomic and Nuclear Science

Jeffrey Charles Bale, TRIUMF Canada; The University of British Columbia Vancouver Canada.
Radu Sorin, Flerov, Russia
Afam Uzorka, KIU Kampala, Uganda.

Abstract

We report on PTMS measurements of $^{31,32}\text{Na}$ and $^{29,34,35}\text{Al}$ performed at TITAN. Mass measurements of several short-lived isotopes at Triumf's Ion Trap for Atomic and Nuclear science were analysed. All of the investigated masses have reduced uncertainties when compared to previous values in the Atomic Mass Evaluation of 2012. Mass excesses for $^{31,32}\text{Na}$ were found to be 12246(14) keV and 18638(37) keV, respectively, with uncertainties being half of the smallest of those currently published in AME. Mass excess of $^{29,34,35}\text{Al}$ were shown to be -18207.77(37) keV, -3000.5(29) keV, and -223.7(73) keV. The mass excess of ^{34}Al has also confirmed the two-neutron separation energy cross over with ^{33}Mg to be 15(10) keV at a $N=21$. The measurements presented in this paper aid in our understanding of the island of inversion

1 Introduction

As the benchmark for accurate and precise mass measurements, PTMS has been repeatedly used to uncover deviations from previous measurements, for Na^{32} , one of the isotopes investigated here, Na^{32} 's values from the TOF technique spans a range of 2:5 MeV with uncertainties varying from 0.1 MeV to 1.3 MeV [1, 2, 3, 4]. However, PTMS also has the ability to reveal smaller, novel features that may have otherwise been looked over due to a lack of resolution. An example of one of these features revealed by PTMS is the crossover of the two neutron separation energy, S_{2n} , found in ^{33}Mg and ^{34}Al , as first discussed at length in [5]. When initially discovered, this crossover was considered to be due to inaccurate mass measurements [5]; however, previous mass measurements performed at TITAN [6, 5], as well as this work have further confirmed the crossover. Large scale nuclear-shell-model calculations [5] indicate that the crossover arises from large gains in correlation energy due to degenerate energy levels. A possible experimental explanation for the seeing this crossover would be the measurement of an isomer [7] that was erroneously assigned to be the ground state. Additional measurements were required to determine the excitation energy of this theoretical isomer. This is the motivation of the mass measurements presented here.

We report on PTMS measurements of $^{31,32}\text{Na}$ and $^{29,34,35}\text{Al}$ performed at TITAN [8]. Particular attention was given to searching for a recently discovered, long-lived isomer of ^{34}Al [7]. Since the excitation energy is unknown, this may affect the understanding of the reported crossover of the two-neutron separation energies of ^{33}Mg and ^{34}Al [5]. Though an isomer was not observed in

this work, we have confirmed the previous measurement of the ground-state mass [5] and, thus, the crossover in the two-neutron separation energy.

2 Experiment

The measurements presented in this work were performed at the ISAC-TRIUMF facility [9] via the ISOL technique. The sodium isotopes were surface-ionized; while aluminium isotopes were ionized via TRILIS [10]. In this experiment, the determined yields ranged from 75 Particles Per Second (PPS) for ^{34}Al , to 2.0×10^6 PPS with ^{29}Al . The singly charged beam was mass separated via the dipole magnet spectrometer with $R \approx 2500$ [11] and then transported at 20 keV to the TITAN facility where it underwent further beam preparation followed by the mass measurement itself. The preparation involved the cooling and bunching of the beam via the TITAN RFQ, and further mass separation by the use of a BNG, and finally dipole cleaning [12] to purify the beam. Once cleaned, the TOF-ICR technique [13] was used to determine the cyclotron frequency, V_c . This frequency is related to the ion's mass m , the ion's charge q , and the magnetic field B of MPET via

$$V_c = \frac{1}{\pi} \frac{q}{m} B. \quad (1)$$

With the TOF-ICR technique, the ion's TOF is measured as a function of the excitation frequency applied to the trap, after which the data are fitted with the analytic line-shape [14], whose centroid corresponds to the cyclotron frequency, as shown in Figure 1. The centroid of this figure corresponds to the cyclotron frequency of $^{34}\text{Al}^+$. In the case of ^{29}Al , a Ramsey excitation scheme [15, 16] was applied with two 100 ms excitation pulses separated by 300 ms.

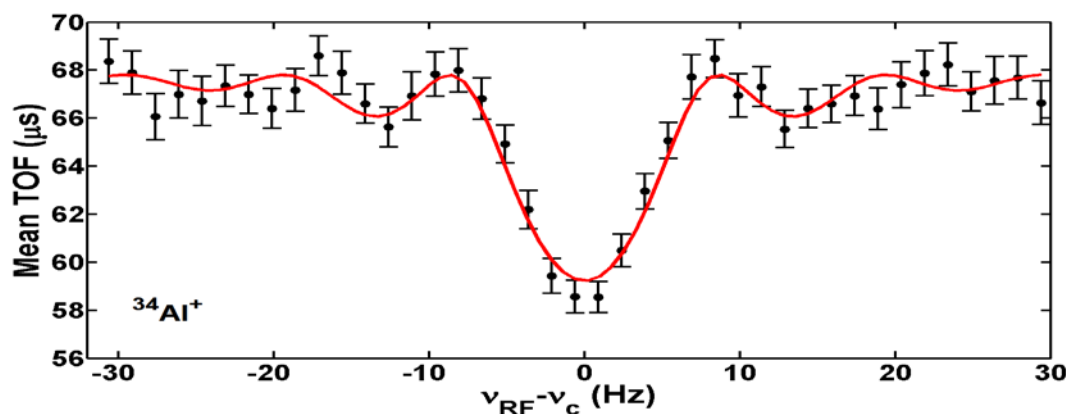


Figure 1: TOF spectrum of ^{34}Al with an excitation time of 100 ms. Here $V_c \approx 1670813$ Hz. The solid curve is the analytic fit [14].

3 Data Analysis

Taking the ratio of frequencies between a reference ion $V_{c,ref}$, and the isotope of interest V_c , allows the magnetic field to be cancelled out as in Equation 2:

$$R = \frac{V_{c,ref}}{2V_c} = \frac{q_{ref}}{q} \cdot \frac{m}{m_{ref}}. \quad (2)$$

By using this cancelling out of magnetic fields, the measurements may be calibrated by bracketing each radioactive ion measurement by reference ion measurements. This bracketing allowed for a linear interpolation of the magnetic field to the time of the radioactive ion's cyclotron frequency being determined. This ratio is, in principle, independent of the magnetic field, and thus, our primary result. The frequency ratios and their statistical uncertainties are shown in Table 1.

We analysed the data to determine both the systematic and statistical uncertainties. Systematic uncertainties [17] including relativistic effects, non-linear fluctuations in the magnetic field, anharmonicities in the trapping potential, and other mass-dependent effects were found to be negligible as compared to statistical uncertainties (relative uncertainties of 10^{-9} vs 10^{-7}).

Species	Reference Ion	T_{ex} (ms)	R	ME_{TITAN} (keV)	ME_{Lit} (keV)	S_{2n} (KeV)
^{31}Na	$^{39}\text{K}^+$	20	1.25636549(62)	12246(14)	12261(23)	657(16)
^{32}Na	$^{39}\text{K}^+$	20	1.2168586(15)	18638(37)	18810(120)	5979(38)
^{29}Al	$^{23}\text{Na}^+$	100- 300- 100	0.793281449(10)	-18207.77(37)	-18209.0(19)	17153.51(37)
^{34}Al	$^{39}\text{K}^+$	50	1.14610225(44)	-2999(12)	-2990.0(72)	8042(15)
^{34}Al	$^{39}\text{K}^+$	71	1.14610245(24)	-3004.4(67)	-2990.0(72)	8048(11)
^{34}Al	$^{39}\text{K}^+$	100	1.14610227(12)	-2999.5(34)	-2990.0(72)	8042.8(93)
^{34}Al	$^{39}\text{K}^+$	50,71, 100	1.14610230(11)	-3000.5(29)	-2990.0(72)	8043.7(92)
^{35}Al	$^{39}\text{K}^+$	50	1.11325817(25)	-223.7(73)	-220(70)	7869(10)

Table 1: Each of the nuclides measured in this paper is presented here, alongside the ion that was used as its reference, the excitation time in MPET T_{ex} , the ratio R, (see Equation 2), mass excesses ME from both this work and literature, as well as the two-neutron separation energy S_{2n} . For $^{31,32}\text{Na}$ and ^{35}Al we compare to AME [18] and for $^{29,34}\text{Al}$ the more recent values in reference [5]. We also used the mass measurements of $^{27,32,33}\text{Al}$ in [5] to calculate the S_{2n} . All species presented in this experiment had a charge state of +1. In the case of ^{29}Al , a 100- 300-100 ms Ramsey excitation [15] was used. This table also presents the combined results of the 50, 71, 100 ms excitation time of ^{34}Al .

These systematic uncertainties were typically two orders of magnitude smaller than statistical (relative uncertainties of 10^{-9} versus 10^{-7}), and thus were insignificant. The uncertainty stemming from ion-ion interactions was determined via a count-class analysis [19] whenever yields allowed. This count class analysis takes into account the detector efficiency ($40 \pm 20\%$), as well as the number of ions detected in the same measurement. The count-class analysis extrapolates using this information to determine the cyclotron frequency of a single ion in the trap. Moreover, reference measurements of $^{39}\text{K}^+$ or $^{23}\text{Na}^+$ were alternated with the radioactive mass measurements. These calibration measurements were within one standard deviation of Atomic Mass Evaluation (AME) and had comparable uncertainties to those of our radioactive ion measurements.

4 Results

Using the frequency ratio in Equation 2, the atomic masses of the species measured were extracted using the AME mass value of the reference [18], as well as the electron binding energy (BE) [20], and the mass of the electron (m_e), this relation to the atomic mass is defined as

$$M = R.M_{ref} - BE - m_e. \tag{3}$$

As the SOI in this experiment were singly charged, the amount of energy to remove a single electron BE, compared to the measurement’s statistical uncertainty, was negligible and could be ignored. A convenient way to describe masses is by the difference between an atom’s mass and the number of present nucleons. This quantity is referred to as the Mass Excess (ME) of the atom, and is defined by Equation 4 where the mass is in units of AMU, and A is the number of nucleons present in atom.

$$ME = (Mass - A) \times 931.49432 \text{ MeV} \tag{4}$$

The resulting ME values are presented in Table 1 alongside the literature values. MEes of ^{31}Na and ^{32}Na were found to be 12246(14) keV and 18638(37) keV, respectively. The uncertainties of these new measurements are half of the smallest currently published in AME. While our measurement of ^{31}Na is 0.6σ from the values in AME, we find a deviation of 1.4σ for ^{32}Na , as shown in Figure 2.

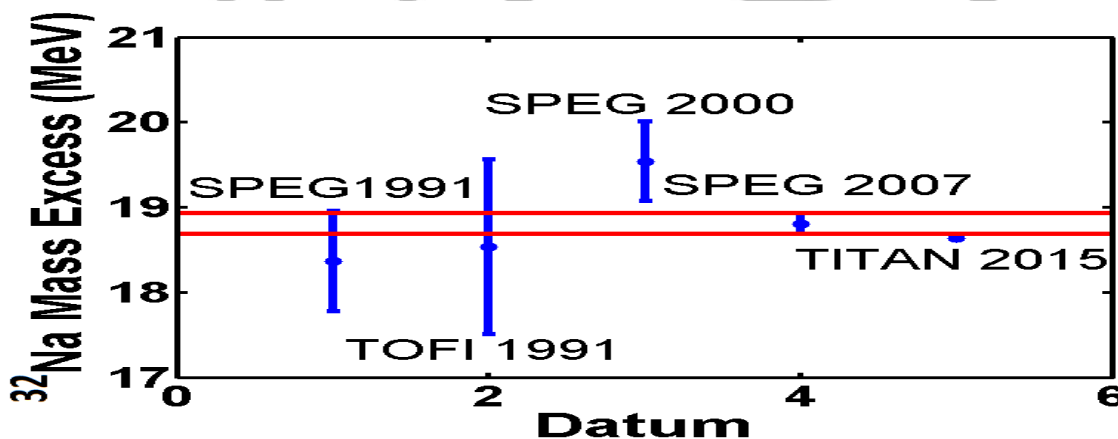


Figure 2: A sample of mass measurements with the horizontal lines centred around the AME indicating the 1σ confidence level. As can be seen our new value, TITAN 2015, disagrees with AME by 1.4σ . Values taken from [2, 21, 4]

The TITAN-measured mass excesses for $^{29;34;35}\text{Al}$ are listed in Table 1. Those of $^{29;34}\text{Al}$ agree with our prior measurements [5] within a 1σ and 2σ uncertainties, but also have lower uncertainties. The ME value of ^{35}Al presented in Table 1 agrees with AME [18] and has an improved precision by a factor of ten over the previous values determined via the TOF technique [1, 2, 3, 4].

During the experiment and data analysis, we paid special attention to ^{34}Al due to the possible presence of a long-lived isomer [7]. Such an isomer could have been produced in the ISAC production target and delivered simultaneously with the ground state. To identify the constituent species in the beam we turned the laser ionization of ^{34}Al on and off. Note that due to Doppler broadening in the ionization region, both the ground state of ^{34}Al and its isomer would be ionized with the same laser-excitation scheme. Stable $^{31}\text{P}^+\text{H}_3$ accounted for at least 75% of the surface-ionized beam. Thus, more than 90% of the beam at the MPET MCP produced with laser ionization was $^{34}\text{Al}^+$. The stable $^{31}\text{P}^+\text{H}_3$ were identified via its V_c in the MPET.

If an isomer were present during the mass measurements, a second resonance feature would be visible in its TOF distribution (see for ex. [22]). In the analysis, we attempted to fit the data with a fitting function for both a single and double resonance; however, no second resonance was observed. Therefore, only one species was identified. In an effort to clarify which nuclear state of ^{34}Al was being measured, we used multiple v excitation times as the isomer and ground state have very different half-lives with the isomer's being 26(1) ms [8] and the ground state of 56:3(5) ms [23]. The various excitation times used were 50 ms, 71 ms, and 100 ms. Due to variations in the ISAC yields, as well as data being taken for ^{34}Al intermittently with other elements, it was not possible to normalize the count rates between the various measurements of ^{34}Al . These variations in yield were observed to change from a fraction of surface-ionized $^{34}\text{Al}^+$ to surface-ionized contaminant ions of $\approx 12\%$ at the start of the experiment to $\approx 3\%$ at the end of the experiment, and as such a comparison of the count rates could not be used to distinguish the ratio of the ground-state to the isomer if a mixture were present. A linear extrapolation of count rates for ^{34}Al was not possible due to a 48 hour period between the first round of measurements of ^{34}Al with an excitation time of 100 ms, and the second round with the excitation time of 50 ms. This gap was due to taking measurements of our other SOI. However, as the shortest excitation time was nearly twice the half-life of the short lived isomer, a maximum of 14% of those delivered from the target station would survive long enough to be observed. This drop in the number of detected isomers is even more apparent with the longer excitation time of 100 ms with a maximum of 4% of the original isomer yield possibly being measured, further lowering our ability to detect it.

In order for TITAN to observe a separation of two species at a difference of FWHM with the longest excitation, 100 ms, the mass difference would need to be as large as 200, keV. At this point, a second TOF resonance would be considered fully resolved. An illustration of fitting with an isomer present is shown in Figure 3 for various isomers to ground state ratios, as well as mass differences. However, as the short excitation scheme used would reduce the quantity of the isomer to 14% of its original value, we do not expect a yield sufficient to distinguish it from the ^{34}Al ground state.

As no second resonance was observed, and since the isomer yield could be at most 14% of our total ^{34}Al yield, it was concluded that only the ground state was in fact, the species measured. The only other known isomeric state [24] was observed via a Coulomb excitation experiment, and its half-life is of the order of nanoseconds.

The measured mass excess of ^{34}Al agrees with that of TITAN's previous measurement of -2990:0(72) keV [5], but with a smaller uncertainty due to better statistics. Using this updated mass excess, two-neutron separation energies were found to overlap for ^{33}Mg and ^{34}Al . The two-neutron separation energy tabulated in Table 1 is defined as:

$$S_{2n}(N,Z) = -m(N,Z) + m(N-2, Z) + 2m_n. \quad (5)$$

Thus, with our observations, the two-neutron separation energy crossover of ^{33}Mg and ^{34}Al at $N = 21$ is confirmed with an overlap of 15(10) keV.

The importance of the aluminium masses derives from their transitional nature as they border the island of inversion. In addition to agreeing with previous measured mass values, the $^{29;34;35}\text{Al}$ values presented here support large-scale nuclear shell model calculations [5], the values of Mg were obtained from [25]. In these predictions, $^{34;35;36}\text{Al}$ have mixed sd and p f nuclear orbitals. The relative gains in correlation energy peak at $N = 21;22$ for the aluminium isotopes, which can be seen in the trend of the two-neutron separation energy flattening from ^{34}Al to ^{36}Al . Figure 4 shows this for Al, and Mg for the $N = 19 - 21$ region, and shows the an overlap at $N = 21$. This overlap is known as the crossover at $N = 21$. The present TITAN measurements are in agreement with this flattening of the $^{34;35}\text{Al}$ two-neutron separation energy. This is significant as the current AME value of ^{36}Al [18] does not agree with this flattening. The TOF mass measurements of ^{36}Al currently span ≈ 0.3 MeV with uncertainties at a maximum of ≈ 0.4 MeV [2, 3, 4]. A discrepancy of approximately 0.5 MeV with the literature value [18] would bring the measured mass in agreement with the calculated value and strongly support the predicted gains in correlation energy [5].

This correlation energy would be due to a neutron pair crossing the $N=20$ shell gap, and occupying close lying orbitals in the p f shell [26]. This is also known as a two-particle-two-hole excitation. The new state is now constructed of the two-particle-two-hole excitations may then lead to a lowering of the ground state energy, leading to the flattening of the $^{21-23}\text{Al}$ two-neutron separation energy.

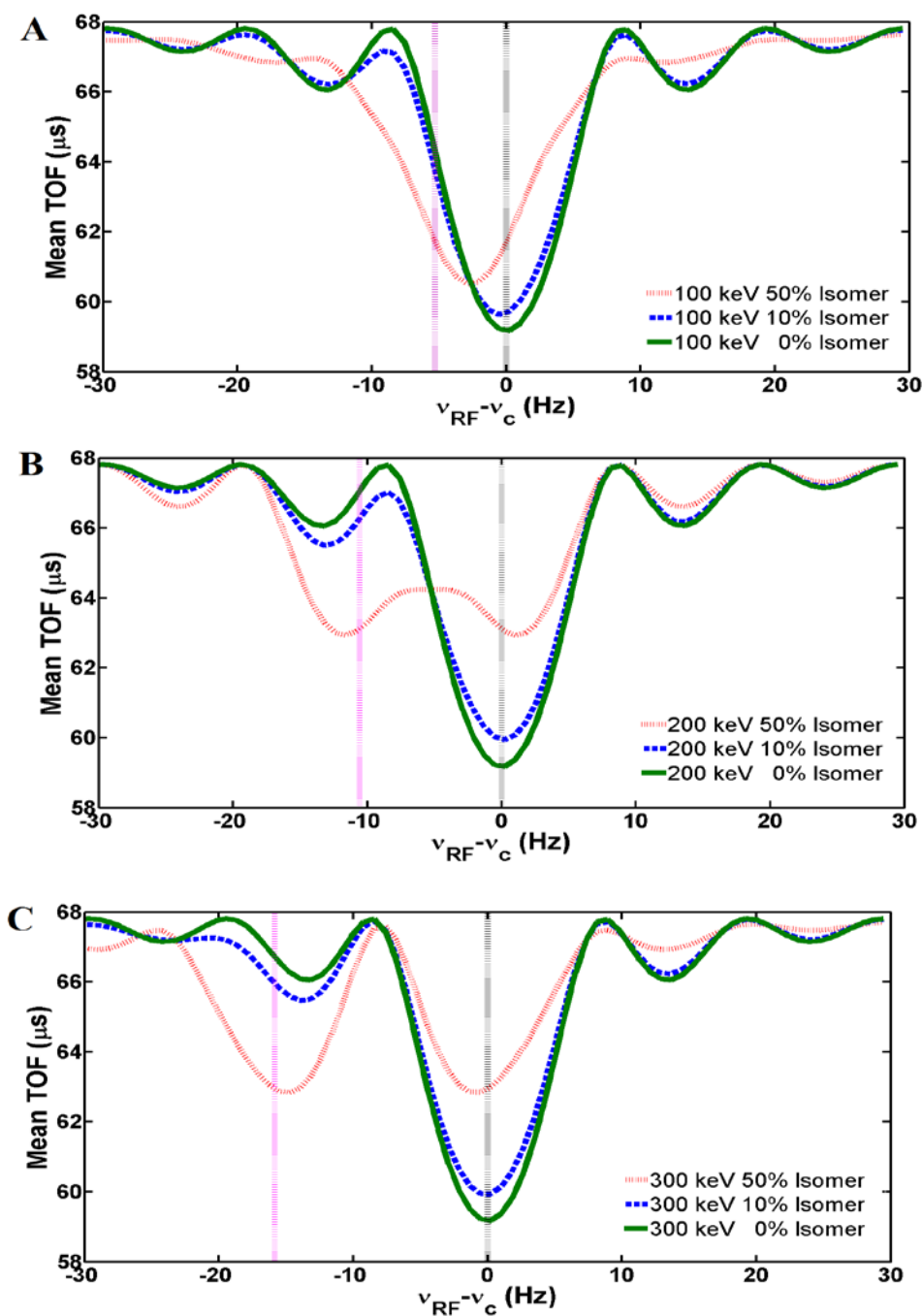


Figure 3: TOF resonance simulations for ^{34}Al for the ground state and isomer with various differences in their masses, and yield ratios. The leftmost vertical line represents the ν_c of the isomer, and the rightmost vertical line represents the ν_c of the ground state, $\nu_c \approx 1670813$ Hz A: a difference of 100 keV and an isomer ratio of anywhere from 50% to 0% of trapped ions. B: a difference of 200 keV was simulated. C: a difference of 300 keV.

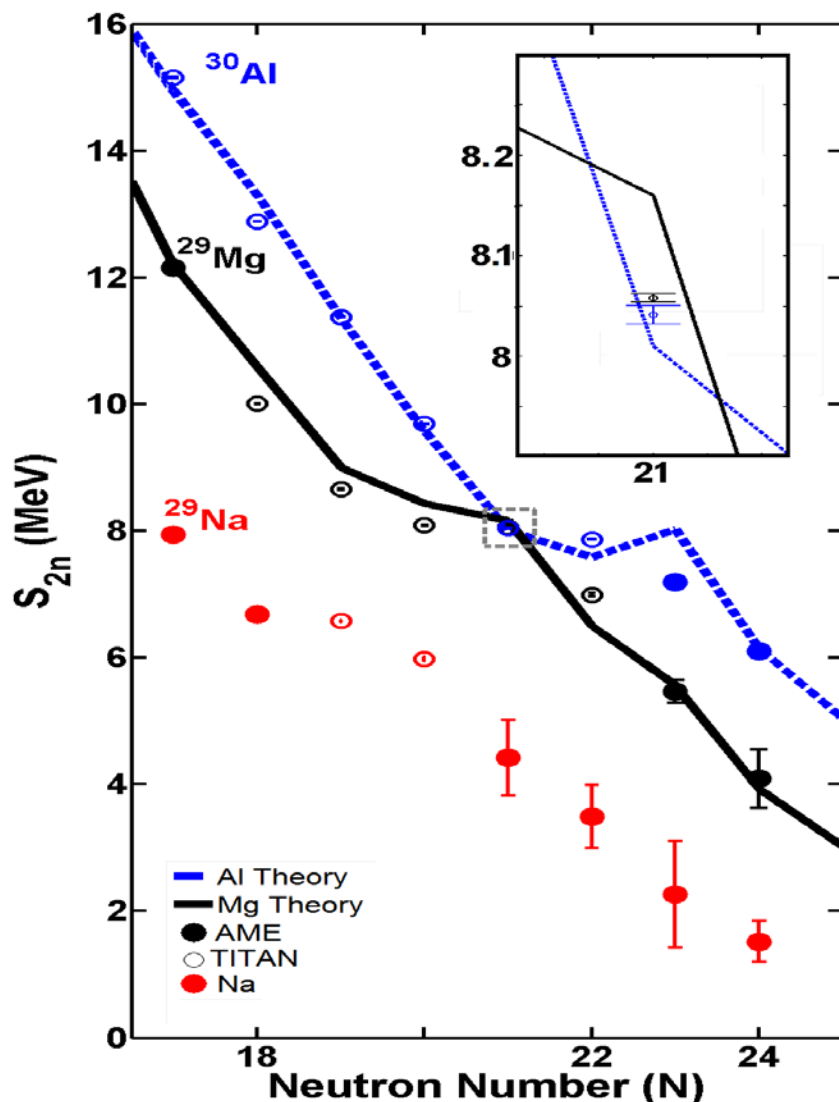


Figure 4: Two-neutron separation energies comparing the experimental results with those from literature, including an expanded view of the $N = 21$ crossovers. Solid circles represent values taken from AME [18], open circles represent values determined by TITAN measurements, triangles represent energies determined using both AME and TITAN measurements together, and lines represent theoretical values [5]. Note that theoretical calculations for Na have yet to be calculated.

6 Conclusions

In this paper, we have presented mass measurements of species that are currently available at ISAC. These mass measurements of $^{31,32}\text{Na}$, as well as $^{29,34,35}\text{Al}$ help aid our understanding in the region of the island of inversion [27], and have joined TITAN's previous mass measurements of the island of inversion now spanning $^{29-32}\text{Na}$, $^{29-34}\text{Mg}$, and $^{29-35}\text{Al}$. The flattening of the S_{2n} from ^{34}Al to ^{36}Al is supported by our investigations, and support the predictions of large correlation gains in $^{34,35}\text{Al}$ [5]. Although extensive efforts were used in the search for an isomer of ^{34}Al , none was observed. This supports the claims in Reference [5] of a crossover in the two-neutron separation energy of the ^{33}Mg and ^{34}Al ground states.

Although the measurements presented in this paper aid in our understanding of the island of inversion, more measurements must be carried out to further our understanding of the inversion mechanism itself. Spin-parity measurements will play a role in investigating the inversion mechanism, and as such spectroscopic information is still needed. The structure of the ^{34}Al is still under debate [5, 7], as its observation has been elusive at radioactive-isotope-beam facilities, and thus far its production has been achieved only via decay from its parent, ^{34}Mg [8]. TITAN has recently demonstrated the capacity to recapture the daughter from a radioactive decay for subsequent mass measurements. The mass of ^{36}Al is now well within TITAN's reach, and its mass may substantiate the predicted gains in correlation energy [5] and the flattening of S_{2n} for $N = 21-23$ observed in the aluminium isotopic chain.

Glossary

Throughout this paper, many acronyms were used. For simplicity, and convenience, each one is defined here

AME: Atomic Mass Evaluation

AMU: Atomic Mass Unit

BNG: Bradbury Nielsen Gate

FWHM: Full Width Half Max

ISAC-TRIUMF: Isotope Separator and ACcelerator at TRIUMF

ISAC: Isotope Separator and ACcelerator

ISOL: Isotope Separator On-Line

ME: Mass Excess

MPET: Measurement Penning Trap

PPS: Particles Per Second

PTMS: Penning Trap Mass Spectrometry

SOI: Species of Interest

TITAN: TRIUMF's Ion Trap for Atomic and Nuclear science

TOF: Time-Of-Flight

TOF-ICR; Time-Of-Flight Ion Cyclotron Resonance

TRILIS: TRIUMF's Resonant Ionization Laser Ion Source

Bibliography

[1] C. D'az, et al. Mapping of the onset of a new region of deformation: The masses of ^{31}Mg and ^{32}Mg . Nuclear Physics A, 394(3):378 – 386, 1983. ISSN 0375-9474.

doi:[http://dx.doi.org/10.1016/0375-9474\(83\)90111-2](http://dx.doi.org/10.1016/0375-9474(83)90111-2). URL

<http://www.sciencedirect.com/science/article/pii/0375947483901112>. Pages 3, 47, 52

[2] N. Orr, et al. New mass measurements of neutron-rich nuclei near $n=20$. Physics Letters B, 258(12):29 – 34, 1991. ISSN 0370-2693. doi:[http://dx.doi.org/10.1016/0370-2693\(91\)91203-8](http://dx.doi.org/10.1016/0370-2693(91)91203-8).

URL <http://www.sciencedirect.com/science/article/pii/0370269391912038>. Pages xiv, 3, 47, 52, 57

- [3] F. Sarazin, et al. Shape coexistence and the $N = 28$ shell closure far from stability. *Phys. Rev. Lett.*, 84:5062–5065, May 2000. doi:10.1103/PhysRevLett.84.5062. URL <http://link.aps.org/doi/10.1103/PhysRevLett.84.5062>. Pages 47, 52, 57
- [4] X. Zhou, X. et al. Direct mass measurements of the neutron-rich isotopes of fluorine through chlorine. *Physics Letters B*, 260(34):285 – 290, 1991. ISSN 0370-2693. doi:http://dx.doi.org/10.1016/0370-2693(91)91613-Z. URL <http://www.sciencedirect.com/science/article/pii/037026939191613Z>. Pages xiv, 47, 52, 57
- [5] A. A. Kwiatkowski, et al. Observation of a crossover of S_{2n} in the island of inversion from precision mass spectrometry. *Phys. Rev. C*, 92:061301, Dec 2015. doi:10.1103/PhysRevC.92.061301. URL <http://link.aps.org/doi/10.1103/PhysRevC.92.061301>. Pages vii, xv, 47, 48, 50, 52, 54, 56, 57, 58, 59
- [6] A. Chaudhuri, et al. Evidence for the extinction of the $n = 20$ neutron-shell closure for ^{32}Mg from direct mass measurements. *Phys. Rev. C*, 88:054317, Nov 2013. doi:10.1103/PhysRevC.88.054317. URL <http://link.aps.org/doi/10.1103/PhysRevC.88.054317>. Pages 47
- [7] F. Rotaru, et al. Unveiling the intruder deformed $0^+ 2$ state in ^{34}Si . *Phys. Rev. Lett.*, 109:092503, 2012. doi:10.1103/PhysRevLett.109.092503. URL <http://hal.in2p3.fr/in2p3-00712670>. Pages 47, 48, 52, 53, 59
- [8] J. Dilling, et al. R. Mass measurements on highly charged radioactive ions, a new approach to high precision with fTITANg. *Int. J. Mass. Spectrom.*, 251(23):198 – 203, 2006. ISSN 1387 3806. doi:doi:10.1016/j.ijms.2006.01.044. URL <http://www.sciencedirect.com/science/article/pii/S1387380606000777>. Pages 48
- [9] P. Delheij, et al. The titan mass measurement facility at triumpf-isac. *Hyperfine Interact.*, 173(1-3):123–131, 2006. ISSN 0304-3843. doi:10.1007/s10751-007-9573-9. URL <http://dx.doi.org/10.1007/s10751-007-9573-9>. Pages 48
- [10] J. Lassen, et al. Laser ion source operation at the triumpf radioactive ion beam facility. *AIP Conference Proceedings*, 1104(1), 2009. Pages xii, 33, 34, 48
- [11] J. Dilling, R. Krücken, and L. Merminga. *ISAC and ARIEL: The TRIUMF Radioactive Beam Facilities and the Scientific Program*, volume 85. Springer, Apr 2014. doi:10.1007/978-94-007-7963-1. URL <http://www.springer.com/gp/book/9789400779624>. Pages 34, 42, 48
- [12] T. Eronen, et al. Preparing isomerically pure beams of short-lived nuclei at fJYFLTRAPg. *Nuclear Instruments and Methods in Physics Research Section B: Beam Interactions with Materials and Atoms*, 266(1920):4527 – 4531, 2008. ISSN 0168-583X.

doi:<http://dx.doi.org/10.1016/j.nimb.2008.05.076>. URL
<http://www.sciencedirect.com/science/article/pii/S0168583X08007696>. Proceedings of the
fXVthg International Conference on Electromagnetic Isotope Separators and Techniques Related
to their Applications. Pages 42, 48

[13] G. Bollen, et al. The accuracy of heavy ion mass measurements using time of flight ion
cyclotron resonance in a penning trap. *Journal of Applied Physics*, 68(9), 1990. Pages 43, 48

[14] M. König, et al. Quadrupole excitation of stored ion motion at the true cyclotron frequency.
Int. J. Mass Spectrom. Ion Processes, 142(12):95 – 116, 1995. ISSN 0168-1176.
doi:[doi:10.1016/0168-1176\(95\)04146-C](https://doi.org/10.1016/0168-1176(95)04146-C). URL
<http://www.sciencedirect.com/science/article/pii/016811769504146C>. Pages iv, xiii, xiv, 40, 41,
42, 43, 48, 49

[15] S. George, et al. Ramsey method of separated oscillatory fields for high-precision penning
trap mass spectrometry. *Phys. Rev. Lett.*, 98:162501, Apr 2007.
doi:[10.1103/PhysRevLett.98.162501](https://doi.org/10.1103/PhysRevLett.98.162501). URL
<http://link.aps.org/doi/10.1103/PhysRevLett.98.162501>. Pages vii, 48, 50

[16] M. Kretzschmar. The Ramsey method in high-precision mass spectrometry with penning
traps: Theoretical foundations. *Int. J. Mass Spectrom.*, 264 (23):122 – 145, 2007. ISSN 1387-
3806. doi:[doi:10.1016/j.ijms.2007.04.002](https://doi.org/10.1016/j.ijms.2007.04.002). URL
<http://www.sciencedirect.com/science/article/pii/S1387380607001649>. Pages 48

[17] M. Brodeur, et al. V. Verifying the accuracy of the fTITANg penning-trap mass
spectrometer. *International Journal of Mass Spectrometry*, 310:20 – 31, 2012. ISSN 1387-3806.
doi:<http://dx.doi.org/10.1016/j.ijms.2011.11.002>. URL
<http://www.sciencedirect.com/science/article/pii/S1387380611004568>. Pages 43,49

[18] G. Audi, et al. The AME2012 atomic mass evaluation. *Chin. Phys. C*, 36(12): 1287–1602,
2012. doi:[10.1088/1674-1137/36/12/002](https://doi.org/10.1088/1674-1137/36/12/002). Pages vii, xv, 3, 50, 51, 52, 54, 56, 57

[19] A. Kellerbauer, et al. From direct to absolute mass measurements: A study of the accuracy
of isoltrap. *Eur. Phys. J. D.*, 22 (1):53–64, 2003. ISSN 1434-6060. doi:[10.1140/epjd/e2002-
00222-0](https://doi.org/10.1140/epjd/e2002-00222-0). URL <http://dx.doi.org/10.1140/epjd/e2002-00222-0>. Pages iv, xiv, 45, 46, 51

[20] A. Kramida, Y. Ralchenko, and J. Reader. National atomic spectra database (version 5.2)
online, 19-Aug-2015 18:46:14 EDT. URL <http://physics.nist.gov/asd>. Pages 51

[21] F. Sarazin, et al. Shape coexistence and the n=28 shell closure far from stability. *Hyperfine
Interactions*, 132(1-4):147–152, 2001. ISSN 0304-3843. doi:[10.1023/A:1011912400725](https://doi.org/10.1023/A:1011912400725). URL
<http://dx.doi.org/10.1023/A3A1011912400725>. Pages xiv, 3, 52

- [22] A. T. Gallant, et al. Highly charged ions in penning traps: A new tool for resolving low-lying isomeric states. Phys. Rev. C, 85:044311, Apr 2012. doi:10.1103/PhysRevC.85.044311. URL <http://link.aps.org/doi/10.1103/PhysRevC.85.044311>. Pages 53
- [23] S. Nummela, et al. Spectroscopy of $^{34,35}\text{Si}$ by β decay: sd - f p shell gap and single-particle states. Phys. Rev. C, 63:044316, Mar 2001. doi:10.1103/PhysRevC.63.044316. URL <http://link.aps.org/doi/10.1103/PhysRevC.63.044316>. Pages 53
- [24] B. V. Pritychenko, et al. Shape coexistence on the boundary of the “island of inversion”: Exotic beam spectroscopy of ^{34}Al . Phys. Rev. C, 63: 047308, Mar 2001. doi:10.1103/PhysRevC.63.047308. URL <http://link.aps.org/doi/10.1103/PhysRevC.63.047308>. Pages 54
- [25] E. Caurier, F. Nowacki, and A. Poves. Merging of the islands of inversion at $n = 20$ and $n = 28$. Phys. Rev. C, 90:014302, Jul 2014. doi:10.1103/PhysRevC.90.014302. URL <http://link.aps.org/doi/10.1103/PhysRevC.90.014302>. Pages 54
- [26] G. Brown and C. Wong. Correlation energy of oxygen 16. Nuclear Physics A, 100:241–247, Jul 1967. doi:10.1016/0375-9474(67)90406-X. URL <http://www.sciencedirect.com/science/article/pii/037594746790406X>. Pages 57
- [27] E. Courant and H. Snyder. Theory of the alternating-gradient synchrotron. Annals of Physics, 3(1):1 – 48, 1958. ISSN 0003-4916. doi:http://dx.doi.org/10.1016/0003-4916(58)90012-5. URL <http://www.sciencedirect.com/science/article/pii/0003491658900125>. Pages 18